

Modeling Random Telegraph Noise Under Switched Bias Conditions Using Cyclostationary RTS Noise

Arnoud P. van der Wel, Eric A. M. Klumperink, L. K. J. Vandamme, and Bram Nauta

Abstract—In this paper, we present measurements and simulation of random telegraph signal (RTS) noise in n-channel MOSFETs under periodic large signal gate-source excitation (switched bias conditions). This is particularly relevant to analog CMOS circuit design where large signal swings occur and where LF noise is often a limiting factor in the performance of the circuit. Measurements show that, compared to steady-state bias conditions, RTS noise can decrease but also increase when the device is subjected to switched bias conditions. We show that the simple model of a stationary noise generating process whose output is modulated by the bias voltage is not sufficient to explain the switched bias measurement results. Rather, we propose a model based on cyclostationary RTS noise generation. Using our model, we can correctly model a variety of different types of LF noise behavior that different MOSFETs exhibit under switched bias conditions. We show that the measurement results can be explained using realistic values for the bias dependency of τ_c and τ_e .

Index Terms—Cyclostationary, large signal excitation, LF noise, MOSFET, random telegraph signal (RTS) noise, simulation, switched biasing.

I. INTRODUCTION

IN CMOS, low-frequency noise is an increasing problem. As device sizes become smaller, low-frequency noise plays a larger role in limiting circuit performance. For robust circuit design it is crucial to understand the noise sources in the devices in detail. Recent work has made clear that random telegraph signal (RTS) noise plays a significant role in the LF noise performance of MOSFETs [1]. Also, it has been demonstrated that LF noise can decrease when a device is subjected to switched bias conditions [2]–[4], which can, for example, be exploited in oscillators [5]. Two authors have proposed models to explain this reduction [6], [7] but their models cannot account for the recent observation [8] that RTS noise in small MOSFETs ($W/L = 0.2 \mu\text{m}/0.18 \mu\text{m}$) can not only decrease, but also *increase* in intensity when these devices are subjected to switched bias conditions. Also, the models in [6] and [7] predict complete disappearance of the LF noise below the switching frequency, which is not consistent with experimental results. In the current paper, we propose a simulation with cyclostationary RTS noise (periodically time variant statistics) to qualitatively explain all such measurement results.

Manuscript received October 10, 2002; revised March 17, 2003. This work was supported by The Netherlands Technology Foundation, STW. The review of this paper was arranged by Editor J. Deen.

A. P. van der Wel, E. A. M. Klumperink, and B. Nauta are with the IC-Design Group, MESA+ Institute, University of Twente, 7500 AE Enschede, The Netherlands.

L. K. J. Vandamme is with the Department of Electrical Engineering, Eindhoven University of Technology, 5600 MB Eindhoven, The Netherlands

Digital Object Identifier 10.1109/TED.2003.813247

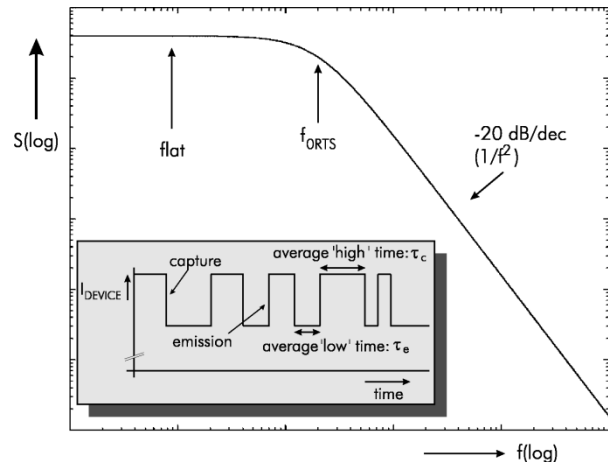


Fig. 1. Time- and frequency-domain representation of a stationary RTS. Time- and frequency-domain representation are equivalent, though time-domain representation contains more information about the RTS.

This paper is organized as follows: In Section II, background information on RTS noise and the traps that are responsible for it is given. In Section III, we describe our cyclostationary RTS noise generation model in detail, and in Section IV, we show how the model can account for the measurement results. Finally, in Section V, conclusions are drawn.

II. RTS AND BIAS-DEPENDENCY

A. Background: Stationary Random Telegraph Signals

In small MOS devices with a low number of free carriers, ($N < 10^4$), LF noise performance is dominated by RTS noise on top of the ever present bulk $1/f$ noise [9], [10]. The LF noise performance of a small device may even be dominated by one single trap. A trap produces so-called RTS noise.

RTS noise (Fig. 1) has two discrete states and switches between the two states at random moments. The RTS noise is observed at the terminals of the device as a discrete fluctuation in drain current. The nomenclature is such that τ_c is the time constant associated with the process of electron capture by a trap and hence, corresponds to the mean time before electron capture occurs. This means that τ_c corresponds to the untrapped state of the electron. The converse holds for τ_e . Since we are considering n-channel MOSFETs where the observed RTS noise is due to traps communicating with the conduction band, the mean time spent in the high current state is τ_c (the capture time) and the mean time spent in the low current state is τ_e (the emission time). A constant τ_c and τ_e mean that the RTS noise is stationary. The power spectrum of such RTS noise is a Lorentzian (Fig. 1):

flat at low frequencies and decaying with -20 db/decade above a particular corner frequency ([11], [1]).

Defining

$$f_{0\text{RTS}} = \frac{1}{2\pi} \left(\frac{1}{\tau_c} + \frac{1}{\tau_e} \right)$$

and

$$\beta = \frac{\tau_c}{\tau_e}$$

we can write

$$S(f) = A^2 \cdot \frac{\beta}{(1 + \beta)^2} \cdot \frac{1}{f_{0\text{RTS}}} \cdot \frac{1}{1 + \frac{f^2}{f_{0\text{RTS}}^2}}.$$

The corner frequency ($f_{0\text{RTS}}$) is determined only by τ_c and τ_e . For a given amplitude A and $f_{0\text{RTS}}$, the LF power spectral density (PSD) depends on β . When $\beta = 1$, the LF PSD will be largest. For strongly asymmetric RTS noise (β far from 1), the LF PSD will be small. Note that the PSD does *not* completely characterize the corresponding RTS. The power spectrum of an RTS only reveals the amplitude of the LF part of the PSD and the corner frequency. One cannot say whether a particular power spectrum is caused by a low-amplitude RTS with $\beta = 1$, or by a large-amplitude RTS with β far from 1. Both signals, though very different in the time domain, can look the same in the frequency domain if they have the same $f_{0\text{RTS}}$. In this paper, we are primarily interested in the effect of a time-variant τ_c and τ_e on the RTS spectrum. *We will assume that the RTS amplitude A is constant*, which is in line with experimental observations.

B. V_{GS} Dependency of τ_c and τ_e

In an n-channel MOSFET, the carrier density n can be varied by changing V_{GS} . According to Shockley-Read-Hall theory, τ_c should decrease with increasing n and τ_e should be independent of n . Hence, we expect τ_c to decrease with increasing V_{GS} and we expect τ_e to be independent of V_{GS} . In practice, however, both τ_c and τ_e show dependency on V_{GS} (energy level of the trap depends on V_{GS}). Several authors [1], [12], [13] have measured τ_e and τ_c as a function of the gate bias voltage in n-channel MOSFETs. They find that as V_{GS} is decreased τ_c increases and τ_e decreases, (the probability of a trap becoming filled decreases and the probability of a trap becoming empty increases). The change in τ is up to two orders of magnitude. In a MOSFET with a large time-variant gate-source voltage, we may therefore expect to find RTS noise with a time variant τ_c and τ_e : cyclostationary RTS noise.

III. CYCLOSTATIONARY RTS NOISE SIMULATION

A. Principle

We want to simulate the generation of RTS noise in a MOSFET that is operated under cyclostationary bias conditions. Since experiments show a strong dependency of τ_c and τ_e on V_{GS} , we incorporate this in our model. We will assume that τ_c and τ_e vary instantaneously with V_{GS} . We designed the simulation so that the simulation results can be directly compared to actual measurements we carried out on $0.2/0.18 \mu\text{m}$ nMOSFETs [8]. For simplicity, we limit ourselves

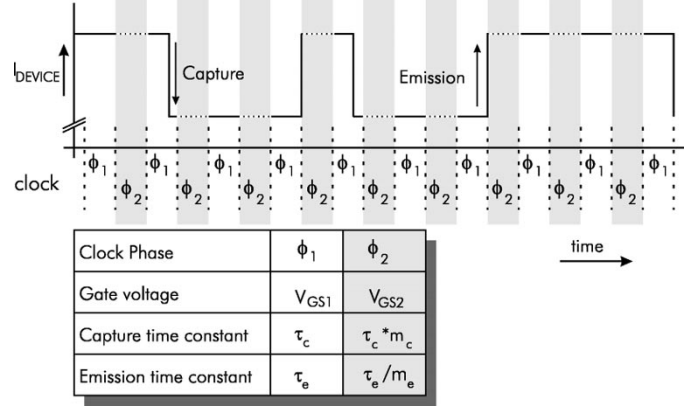


Fig. 2. Cyclostationary RTS has periodically varying τ_c and τ_e that directly depend on V_{GS} . This is the case in MOSFETs where the gate bias is periodically cycled between two values V_{GS1} and V_{GS2} .

to the case where the gate bias V_{GS} is periodically switched between two states (an 'on' state ϕ_1 and an 'off' state ϕ_2) with a 50% duty cycle. Both the drain-source voltage V_{DS} and the bulk-source voltage V_{BS} are kept constant. The two bias states that we periodically alternate between correspond to two different gate voltages and hence, different τ_c and τ_e for the RTS noise generating traps in the device. This is shown in Fig. 2; V_{GS1} corresponds to the "on" state of the device, and V_{GS2} corresponds to the "off" state of the device. We have called the steady-state RTS time constants τ_c and τ_e and have modeled the "off" state time constants as $\tau_c * m_c$ and τ_e / m_e where m_c and m_e are parameters that are to be determined. When m_c and m_e are unequal to 1, the parameters of the RTS (τ_c and τ_e) vary periodically, and the RTS is therefore by definition cyclostationary.

Obviously, when cycling the gate bias, the drain current I_d of the device also changes, and with it, the visibility of the trap at the terminals of the device: When the device is "on," the effect of the trap is visible as a fluctuation in I_d and when the device is "off," I_d is negligible and the behavior of the trap is not visible in the drain current. This is shown in Fig. 3(a): The cyclostationary RTS is modulated by a square wave. The drain current of the device, I_d , [Fig. 3(a)], can be considered as a superposition of two signals: a large square wave with an amplitude of I_L [deterministic; Fig. 3(b)], and a small modulated cyclostationary RTS with an amplitude $I_H - I_L$. [stochastic; Fig. 3(c)]. It is crucial to realize that the RTS continues to exist even at times when we cannot directly observe it! The deterministic current component of Fig. 3(b) contributes a series of δ -functions in the output power spectrum. (At 0 Hz, $\pm f_{\text{switch}}$, $\pm 3f_{\text{switch}}$, $\pm 5f_{\text{switch}}$, etc.) The measurement setup suppresses it as much as possible. The stochastic current component of Fig. 3(c), however, is interesting: it is the modulated, cyclostationary RTS noise that we are after. In the frequency domain, it contributes a series of aliases around harmonics (again: around 0 Hz, $\pm f_{\text{switch}}$, $\pm 3f_{\text{switch}}$, $\pm 5f_{\text{switch}}$, etc.) of the modulating frequency. Using the spectrum analyzer, the dc alias (around 0 Hz) of this signal is measured.

The simulation is designed to produce the signal of Fig. 3(c). This is done by generating a cyclostationary RTS (This models the internal stochastic process; we use a single factor $m =$

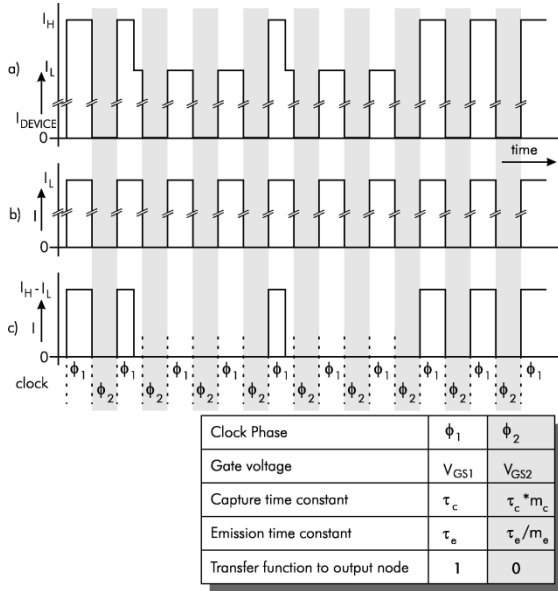


Fig. 3. Cyclostationary, modulated RTS. (a) Total drain current of the device that is cycled between V_{GS1} and V_{GS2} . (b) and (c) Isolate the deterministic and stochastic components of this current, respectively.

$m_c = m_e$ to model the change in τ_c and τ_e , which is then modulated by a square wave. This models the effect of switching on the visibility of the RTS.) The modulated dc drain current [Fig. 3(b)] is not simulated as we are not interested in it.

Note that the simulation presented here is more subtle than the method suggested by Tian and El Gamal [7]. Their calculation is based on the assumption that when the MOSFET is turned “off,” $\tau_c \rightarrow \infty$ and $\tau_e \rightarrow 0$; or in terms of our model: m_c and $m_e \rightarrow \infty$. They correctly note that their method underestimates the noise coming from the device in actual measurements. Their model cannot account for the very variable noise reduction that is observed in different devices, neither can it explain that the LF noise of a number of devices *increases* when subjected to switched bias conditions.

B. Implementation

The simulator was implemented in MATLAB. In general, the transition probabilities per unit time are defined as [11]:

$$P_{\text{capture}}(V_{GS}(t)) = \frac{dt}{\tau_c(V_{GS}(t))}$$

and

$$P_{\text{emission}}(V_{GS}(t)) = \frac{dt}{\tau_e(V_{GS}(t))}.$$

Since we use a time-discrete simulator, (with a constant sample time T_{sample}), we need to substitute T_{sample} in place of dt :

$$P_{\text{capture}}(V_{GS}(t)) = \frac{T_{\text{sample}}}{\tau_c(V_{GS}(t))} \quad [\text{sample}^{-1}]$$

and

$$P_{\text{emission}}(V_{GS}(t)) = \frac{T_{\text{sample}}}{\tau_e(V_{GS}(t))} \quad [\text{sample}^{-1}].$$

Due care is taken that the time-discrete nature of the simulation does not introduce significant errors; i.e., P_{capture} and

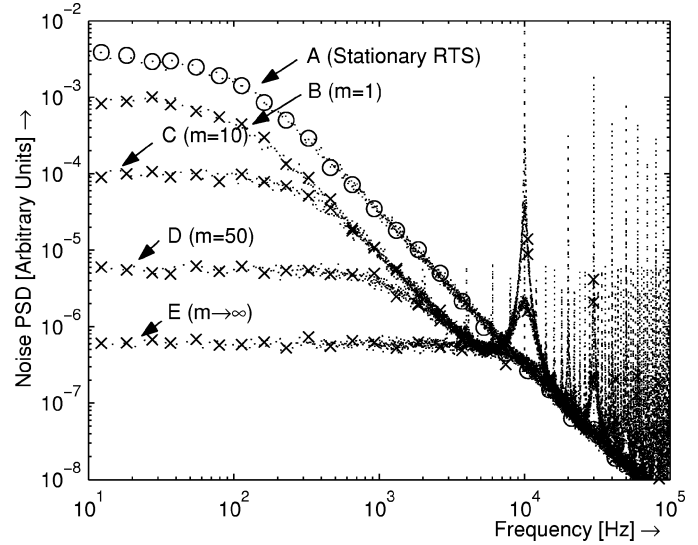


Fig. 4. Simulation highlights the difference between simply modulating an RTS and making it cyclostationary. Modulating the RTS gives a 6 dB decrease in LF noise PSD; making it cyclostationary gives a far larger (and variable) decrease.

$P_{\text{emission}} \ll 1$ [sample⁻¹] and that for each simulation run, an adequate number of transitions is generated to produce statistically significant results. For consistency with the measurements, the lower frequency is chosen to be 10 Hz. The switching frequency is 10 kHz. The sample rate of the simulation is an order of magnitude larger than the highest frequency of interest. To produce a smoother plot, the simulation is carried out a number of times and the results are averaged.

C. Validation of the Simulator

We can now explore the effect of various parameters on the spectrum of the (cyclostationary) RTS. Some simulation results are plotted in Fig. 4: A is the PSD of a stationary RTS for $\beta = 1$. ‘B’ shows the effect of *only modulating* this RTS ($m = m_c = m_e = 1$). As predicted by basic modulation theory [14], the LF PSD has decreased by a factor 4 (6 dB). Apart from the clearly visible LF spectrum, an alias of this spectrum is visible around the switching frequency and its odd multiples, as expected. We now make the modulated RTS cyclostationary: m_c and $m_e \neq 1$. Curve C shows the PSD of the cyclostationary RTS with $m = m_c = m_e = 10$. Curve D shows the PSD for $m = m_c = m_e = 50$ and curve E shows the PSD when m_c and $m_e \rightarrow \infty$. This is the limiting case, where in the “off” state $\tau_c \rightarrow 0$ and $\tau_e \rightarrow \infty$. Curve E has the lowest LF PSD. It corresponds to the method of [6] and [7].

In contrast, our model is able to explain the variable noise reduction that is seen in measurements. Our model can also account for increased LF noise in a MOSFET under switched bias conditions. To illustrate this, we perform a simulation with an asymmetric RTS; $\beta = 0.02$. The results are shown in Fig. 5. The stationary RTS looks much like any other stationary RTS, and the modulated RTS ($m_c = m_e = 1$) brings no surprises either. The interesting curve here is the one where $m_c = m_e = 10$, for which the LF PSD is seen to rise *above* the PSD of the stationary RTS. For much larger values of m_c and m_e , the LF PSD drops once more.

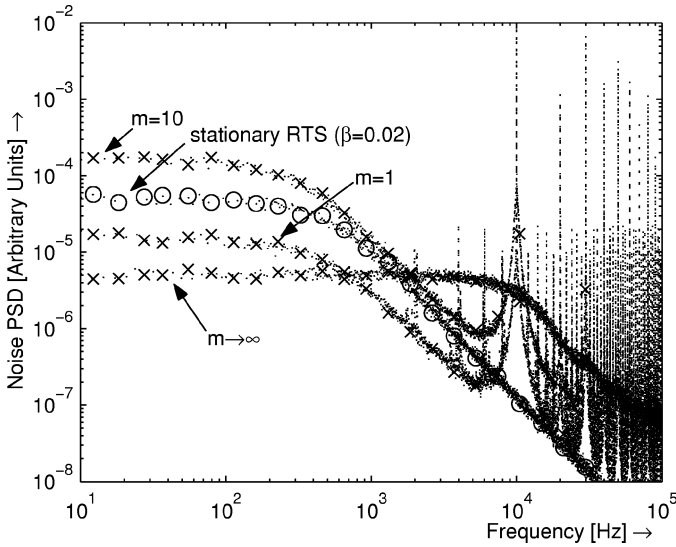


Fig. 5. Generation of cyclostationary RTS starting with asymmetric RTS. An asymmetric RTS can give an LF noise increase when the RTS is made cyclostationary.

In the next section, we will show that the model can reproduce the measurement results by fitting β , m_c and m_e to the measurement results. Before we do that, however, we will examine the measurement results in more detail.

IV. COMPARISON OF MEASUREMENTS TO SIMULATION

In this section, we will show that our cyclostationary RTS generation model can reproduce a number of measurement results. First of all, a measurement with a varying β is carried out by varying the V_{GS} of a single device (Section IV-A), and secondly, a number of randomly selected devices from the same wafer, exhibiting widely varying noise performance, are measured (Section IV-B). Noise measurements were carried out on minimal-size n-channel MOSFETs from a $0.18 \mu\text{m}$ process. Device size (W/L) was $0.2/0.18 \mu\text{m}$. *Steady-state* noise measurements are performed by applying a constant bias voltage to the gate. *Switched bias* noise measurements are carried out by subjecting the device to a 50% duty cycle square wave; i.e., 50% of the time “on,” (V_{GS} same as in the steady-state case), and 50% of the time “off” ($V_{GS} = 0 \text{ V}$). The switching frequency is 10 kHz. For details of the measurement, the reader is referred to [8] and [15].

A. Measurement With Variable V_{GS}

First of all, a measurement was carried out on a single device that was selected for having a very visible RTS. We stepped the V_{GS} of this device through three different values: One where the trap was observed to be approximately half-filled [$\tau_c \approx \tau_e$, Fig. 6(b)], one where it was observed to be mostly full [$\beta \approx 0.3$, Fig. 6(a)], and one where it was observed to be mostly empty ($\beta \approx 10$, Fig. 6(c)). For each V_{GS} , a steady-state bias and a switched bias measurement was carried out. For all measurements, the RTS amplitude at the drain was observed to remain constant in the steady-state case, as well as in the switched bias case. Hence, the difference in the amplitude of the measured

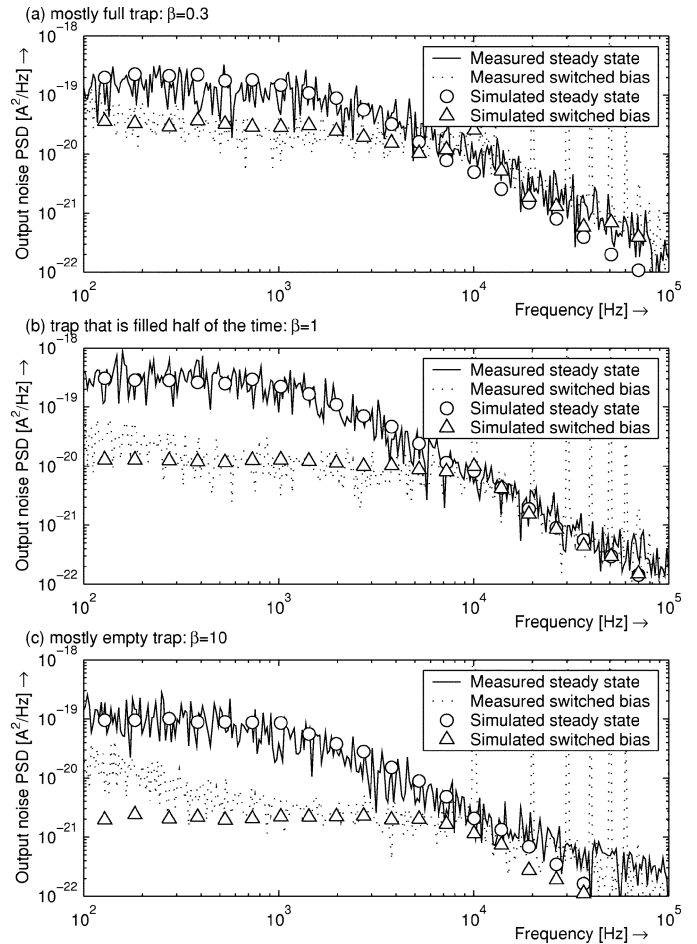


Fig. 6. Different types of RTS noise in a single MOST can also be explained very well using the cyclostationary RTS noise model.

spectra is attributed to differences in the time domain behavior of the RTS.

The measurement results can all be modeled using our cyclostationary RTS noise generation model. First of all, the steady-state simulations are fitted to the steady-state measurement results. Correspondence between simulation and measurement is achieved when, in the simulator, f_{ORTS} is set to 1.5 kHz and β is chosen as 0.3, 1, and 10 for measurements (a), (b), and (c), respectively,¹. The simulated steady-state results are shown as \circ in the figure. To fit the model to the switched bias results, $m_c = m_e = 12$ was chosen. The simulated switched bias results are shown as \triangle in the figure. As can be seen, the steady-state spectra are not as sensitive to variation in β as the switched bias spectra. Thus, after fitting the steady-state results with varying β s, a single assumption ($m = 12$) is adequate to coarsely model all three switched bias results. The only difference between the simulation results for Fig. 6(a)–(c) is in the β of the RTS that is being modeled.

Of course, if more information on the exact bias dependence of τ_c and τ_e is available, the model can be further refined. For

¹Note that what happens in the measurement is slightly more complex than in the simulation, as by changing the β of the traps by varying the V_{GS} , the f_{ORTS} will also change slightly. This, however, is not a strong effect. Note also that in all three measured spectra, the switched bias noise spectrum rises again at low frequencies. This is caused by additional slow RTS noise in the device that is not modeled here.

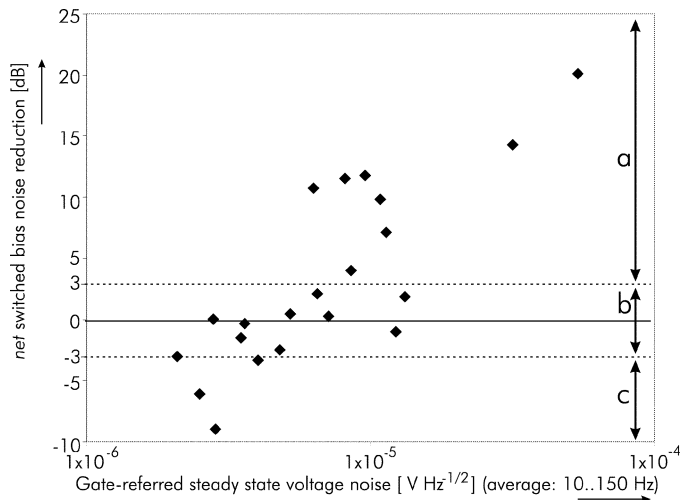


Fig. 7. Net switched bias noise reduction versus steady-state noise power for randomly selected devices: Noise reduction varies and in some cases noise increases.

such refinement, detailed time-domain parameter extraction of the RTS is required. This is the subject of further research.

B. Measurement of 21 Different Devices

Next, 21 nominally identical devices (selected at random) over the whole wafer were measured. These different devices were found to exhibit widely varying RTS noise, in terms of amplitude, f_{ORTS} and β .

The measurement results are plotted in Fig. 7, which shows steady-state noise along the x -axis versus the switched bias noise reduction along the y -axis. The steady-state noise (x -axis) is expressed as average gate-referred noise [$\text{V Hz}^{-1/2}$] in a measurement band from 10 to 150 Hz. The net switched bias noise reduction (y -axis) is measured by subjecting the device to switched bias conditions. In this state, the average LF noise power is again measured from 10 to 150 Hz. The difference between the steady-state noise measurement and the switched bias noise measurement, corrected for the modulation effect (6 dB), is the noise reduction² that is plotted along the y -axis.

In Fig. 7, we can identify three different classes of devices, a, b, and c. The LF noise properties of these different devices are summarized in Table I. In Figs. 8–10, the noise spectrum of one device from each category is examined, and in each case, a stationary RTS noise simulation and a corresponding cyclostationary RTS noise simulation is shown to come into close qualitative agreement with the measured data for the steady-state noise measurement and the switched bias noise measurement respectively. The parameters of the RTS noise simulation for each case are given in Table I.

In each of the Figs. 8–10, a calculated line for the bulk silicon $1/f$ noise is shown, with α_H chosen as 10^{-6} . This is a realistic value for bulk Si [16], and represents the level of bulk $1/f$ noise we would expect in the measurement. It can be seen that the noise we measured is RTS noise, not the bulk $1/f$ noise. In each figure, the output-referred noise PSD is plotted. This

²This is comparable to the LF difference between curve B and curve C, D, or E in Fig. 4.

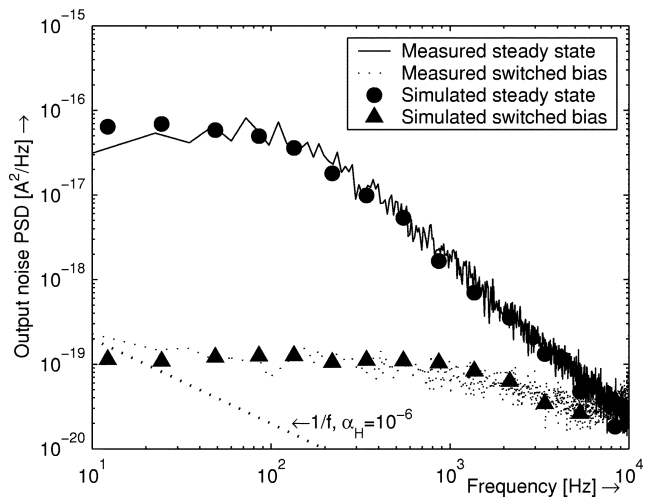


Fig. 8. Measurement and simulation result showing strong decrease in LF noise under switched bias conditions.

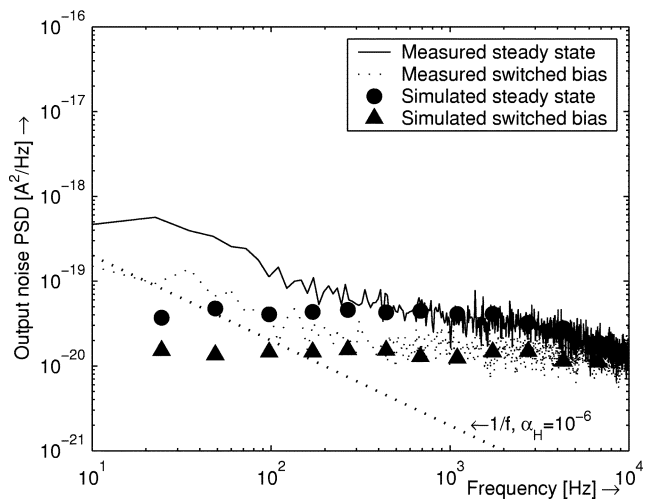


Fig. 9. Measurement and simulation result showing no change in LF noise PSD when the device is subjected to switched bias conditions.

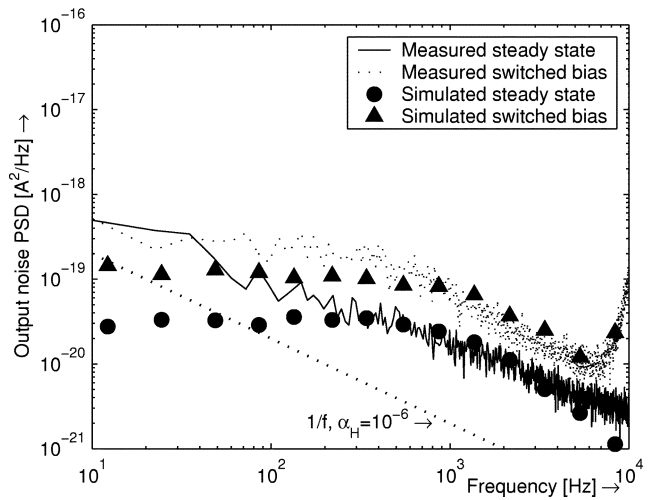


Fig. 10. Measurement and simulation result showing an increase in LF noise when the device is subjected to switched bias conditions.

can be referred to the gate by dividing by the g_m of the device (130 $\mu\text{A/V}$). In Figs. 9 and 10, The measured switched bias

TABLE I
DEVICES OF FIG. 7 CAN BE GROUPED INTO THREE CATEGORIES

Device Category	a	b	c
LF noise under switched biasing	Decrease > 3 dB	No change	Increase > 3 dB
Location in fig. 7	Upper right	Middle	Lower left
RTS simulation: f_o [Hz]	150	5 k	1.5 k
RTS simulation: β	1	0.3	0.02
RTS simulation: $m_c (=m_e)$	50	10	50
Measurement and simulation shown in fig.	8	9	10

spectrum exhibits a rise at low frequencies. This is due to additional slow traps in the device or bulk $1/f$ noise and is not modeled. In Fig. 10, both the switched bias measurement result and the simulation show a rise in the PSD close to the switching frequency. This is the first alias of the noise spectrum around the switching frequency. (This is clearly visible in Fig. 4 as well.)

C. Discussion

When applying switched biasing to a transistor in which noise behavior is dominated by the effect of a single trap, several different types of behavior are seen. Two experiments have been carried out.

In the first experiment, different β s are generated in a single MOSFET by varying V_{GS} . The variation in β has an influence on the steady-state noise spectrum, and a strong effect on the switched bias noise spectrum. In the simulation, we use the same β as observed in the experiments after which we only need to choose the appropriate m_c and m_e (in this case, they are equal) to fit the model to the experimental results.

In the second experiment, different β s are found in different nominally identical devices on the same wafer. In the same way as in the first experiment, cyclostationary RTS noise simulation is able to model the trends in the measurement results. Depending on the parameter β of the trap in question, the LF noise of the device is seen to go down, go up or not change significantly. The two extreme possibilities are highlighted:

- If β is close to 1 in the steady state, (upper righthand corner of Fig. 7) then switched biasing will strongly reduce the noise coming from the device.
- If β is much smaller than 1 in the steady state, (lower left-hand corner of Fig. 7) switched biasing can cause a modest increase in the noise coming from the device. Such a trap is mostly filled in the steady state, and applying switched biasing to the device will cause it to be periodically emptied, thereby increasing its contribution to the LF noise PSD. The traps with β deviating far from 1 are those with a rather low steady-state LF noise PSD. The simulation corresponds to the measurements in this respect.

Of course, the simulation results are not identical to the measurement results in every possible aspect. A link to the physical parameters of the traps in the MOSFETs would greatly aid further insight. However, the strength of the simulation presented here is that a wide range of observations can be explained using

a single, physically realistic assumption, namely that the τ_c and τ_e of a trap in a MOSFET are bias dependent³.

V. CONCLUSION

We propose a simple model in which bias-dependency of τ_c and τ_e for large signal periodic excitation is taken into account, resulting in cyclostationary RTS noise. Using realistic values for the bias-dependency of τ_c and τ_e , the model fits correctly to a variety of switched bias RTS noise measurements.

It is possible to qualitatively model different types of experimentally observed noise spectra by introducing the same type of τ change in each simulation run: In all cases, the capture time constant τ_c is increased, the emission time constant τ_e is decreased, (this is consistent with measured steady-state bias dependency of τ_c and τ_e) and depending on the specific parameter β (τ_c/τ_e) of the trap in question, the LF noise PSD of the device will change. It may show a variable decrease or even an increase.

In circuit design, designers need to consider the worst case noise performance of the device. The model shows why it is only the devices with a low steady-state noise that exhibit a noise increase under switched bias conditions. For a noise increase under switched bias conditions, the time constants of the trap need to be strongly asymmetric to start with, and this means a relatively low steady-state noise PSD. Applying switched biasing as a circuit technique will therefore improve the performance of the noisiest devices, whilst any increase in noise will occur in less noisy devices, and hence be harmless.

The model presented here is not only relevant to circuit design where accurate characterization of MOSFET noise sources is of critical importance, but also gives useful insight into the physical characteristics of traps that generate RTS noise.

ACKNOWLEDGMENT

The authors would like to acknowledge S. Gierkink for the first prototypes of the simulator, and the reviewers for their constructive comments to improve the paper.

REFERENCES

- [1] M. J. Kirton and M. J. Uren, "Noise in solid-state microstructures: A new perspective on individual defects, interface states and low-frequency ($1/f$) noise," *Adv. Phys.*, vol. 38, no. 4, pp. 367–468, 1989.
- [2] I. Bloom and Y. Nemirovsky, " $1/f$ noise reduction of metal-oxide-semiconductor transistors by cycling from inversion to accumulation," *Appl. Phys. Lett.*, vol. 58, pp. 1664–1666, Apr. 1991.
- [3] B. Dierickx and E. Simoen, "The decrease of 'random telegraph signal' noise in metal-oxide-semiconductor field-effect transistors when cycled from inversion to accumulation," *J. Appl. Phys.*, vol. 71, pp. 2028–2029, Feb. 1992.
- [4] S. L. J. Gierkink, E. A. M. Klumperink, A. P. van der Wel, G. Hoogzaad, A. J. M. van Tuijl, and B. Nauta, "Intrinsic $1/f$ device noise reduction and its effect on phase noise in CMOS ring oscillators," *IEEE J. Solid-State Circuits*, vol. 34, pp. 1022–1025, July 1999.
- [5] E. A. M. Klumperink, S. L. J. Gierkink, A. P. van der Wel, and B. Nauta, "Reducing MOSFET $1/f$ noise and power consumption by switched biasing," *IEEE J. Solid-State Circuits*, vol. 35, pp. 994–1001, July 2000.

³In modeling the experimental results, we have in each case assumed $m_c = m_e$. There is no strong physical basis for this assumption, but it offers a reasonable fit to the experimental data. Further refinement of the model (eg. $m_c \neq m_e$) seems to be sensible only if more detailed experimental results are available.

- [6] S. L. J. Gierkink, "Control linearity and jitter of relaxation oscillators," Ph.D. dissertation, Univ. Twente, Enschede, The Netherlands. [Online] Available: icd.el.utwente.nl/publications/icpub1999/dis_sgierkink.pdf, 1999.
- [7] H. Tian and A. El Gamal, "Analysis of $1/f$ noise in switched MOSFET circuits," *IEEE Trans. Circuits Syst. II*, vol. 48, pp. 151–157, Feb. 2001.
- [8] A. P. van der Wel, E. A. M. Klumperink, and B. Nauta, "'Switched biasing' affects $1/f$ noise and random telegraph signals in deep-submicron MOSFET's," *Electron. Lett.*, vol. 37, no. 1, pp. 56–57, Jan. 2001.
- [9] T. G. M. Kleinpenning, "On $1/f$ noise and random telegraph noise in very small electronic devices," *Phys. B*, vol. 164, pp. 331–334, 1990.
- [10] L. K. J. Vandamme, D. Sodini, and Z. Gingl, "On the anomalous behavior of the relative amplitude of RTS noise," *Solid State Electron.*, vol. 42, no. 6, pp. 901–905, June 1998.
- [11] S. Machlup, "Noise in semiconductors: Spectrum of a two-parameter random signal," *J. Appl. Phys.*, vol. 21, no. 3, pp. 341–343, Mar. 1954.
- [12] N. B. Lukyanchikova, M. V. Petrichuk, and N. P. Garbar, "Asymmetry of the RTS's capture and emission kinetics in nMOSFETS processed in a $0.35\ \mu\text{m}$ CMOS technology," in *Proc. 14th Int. Conf. Noise Phys. Syst. 1/f Fluctuations (ICNF)*, Leuven, Belgium, 1997, pp. 232–235.
- [13] Z. Shi, J. Miéville, and M. Dutoit, "Random telegraph signals in deep submicron n-MOSFET's," *IEEE Trans. Electron Devices*, vol. 41, pp. 1161–1168, July 1994.
- [14] H. Taub and D. L. Schilling, *Principles of Communication Systems*. New York: McGraw-Hill, 1986, sec. 1–3 and 1–6.
- [15] A. P. van der Wel, E. A. M. Klumperink, S. L. J. Gierkink, R. F. Wassenaar, and H. Wallinga, "MOSFET $1/f$ noise measurement under switched bias conditions," *IEEE Electron Device Lett.*, vol. 21, pp. 43–46, Jan. 2000.
- [16] R. H. M. Clevers, "Volume and temperature dependence of the $1/f$ noise parameter α in Si," *Phys. B*, vol. 154, pp. 214–224, 1989.



Arnoud P. van der Wel (S'00) was born in Bunschoten, The Netherlands, in 1974. He received the M.Sc. degree (*cum laude*) in electrical engineering from the University of Twente, Enschede, The Netherlands, in 1997. He is a qualified physics teacher and is currently working toward the Ph.D. degree with the IC-Design Group of the University of Twente.

The focus of his research is the reduction of LF noise in MOSFETs and the application of noise reduction techniques to RF circuit design.



Eric A. M. Klumperink (M'98) was born on April 4, 1960, in Lichtenvoorde, The Netherlands. He received the B.Sc. degree in 1982 and the Ph.D. degree from the University of Twente, Enschede, The Netherlands, in 1997.

In 1984, he joined the Faculty of Electrical Engineering, University of Twente. He is currently an Assistant Professor and is involved in teaching and research with the IC-Design Laboratory, Faculty of Electrical Engineering, and the IC-Design Theme of the MESA+ Research Institute. His research interest

is in design issues of high-frequency CMOS circuits, especially for front-ends of integrated CMOS transceivers.



L. K. J. Vandamme received the B.Sc. degree in electrical engineering from H.T.I. Oostende, Oostende, Belgium, in 1965, the M.Sc. degree (*cum laude*) from the Delft University of Technology (DUT), Delft, The Netherlands, in 1971, and the doctorate degree from the Eindhoven University of Technology (EUT), Eindhoven, The Netherlands in 1976.

Since September 1965, he held full time positions, respectively, at the Nuclear Reactor Institute, the Department of Electrical Engineering and the Department of Mechanical Engineering, DUT, and the Department of Electrical Engineering, EUT, since 1972. He was an invited visiting professor with the University of Montpellier, France, during 1981–1982, 1986–1987, and 1992, at the University of Bordeaux in 1998, and at the University of Uppsala in 1999 and 2001. He has done research on $1/f$ noise in metals, semiconductors, organic semiconductors and insulators (optical fibers), electrical contacts, and devices, especially MOSFETs, MESFETs, MODFETs, (laser) diodes, solar cells, and bipolar transistors. He has written and collaborated on more than 160 scientific journal and conference publications. His current interest is on low-frequency noise as a diagnostic tool for reliability and quality assessment in materials, contacts, and devices.



Bram Nauta (S'89–M'91) was born in Hengelo, The Netherlands, in 1964. He received the M.Sc. degree (*cum laude*) in electrical engineering and the Ph.D. degree on the subject of analog CMOS filters for very high frequencies, both from the University of Twente, Enschede, The Netherlands, in 1987 and 1991, respectively.

In 1991, he joined the Mixed-Signal Circuits and Systems Department, Philips Research, Eindhoven, The Netherlands, where he worked on high-speed AD converters. From 1994, he led a research group in the same department, working on "analog key modules." In 1998 he returned to the University of Twente, as full professor heading the Department of IC Design group in the MESA+ Research Institute and the Department of Electrical Engineering. His current research interest is analog CMOS circuits for transceivers. He is also a part-time consultant in industry. In 2001 he cofounded Chip Design Works. His Ph.D. thesis was published as a book: *Analog CMOS Filters for Very High Frequencies* (Boston, MA: Kluwer, 1993). He holds eight patents in circuit design.

Dr. Nauta received the "Shell Study Tour Award" for his Ph.D. work. From 1997 to 1999, he served as Associate Editor of the IEEE TRANSACTIONS ON CIRCUITS AND SYSTEMS —II, and in 1998, he served as Guest Editor for the IEEE JOURNAL OF SOLID-STATE CIRCUITS. In 2001, he became an Associate Editor for the IEEE JOURNAL OF SOLID-STATE CIRCUITS. He is a member of the technical program committee of ESSCIRC and ISSCC.